Paramagnetic $LaCoO_3$: A Highly Inhomogeneous Mixed Spin-State System

D. Takegami,[1] A. Tanaka,[2] S. Agrestini,[1,*] Z. Hu,[1] J. Weinen,[1] M. Rotter,[1] C. Schüßler-Langeheine,[3,†] T. Willers,[3] T. C. Koethe,[3] T. Lorenz,[3] Y. F. Liao,[4] K. D. Tsuei,[4] H.-J. Lin,[4] C. T. Chen,[4] and L. H. Tjeng[1]

[1]*Max Planck Institute for Chemical Physics of Solids, Nöthnitzer Straße 40, 01187 Dresden, Germany*
[2]*Department of Quantum Matter, ADSM, Hiroshima University, Higashi-Hiroshima 739-8526, Japan*
[3]*II. Physikalisches Institut, Universität zu Köln, Zülpicher Straße 77, 50937 Köln, Germany*
[4]*National Synchrotron Radiation Research Center, 101 Hsin-Ann Road, Hsinchu 30077, Taiwan*

(Received 1 February 2022; revised 5 December 2022; accepted 6 February 2023; published 13 March 2023)

We investigate the electronic structure of $LaCoO_3$ across the gradual spin-state and insulator-to-metal transitions using bulk-sensitive hard x-ray photoelectron and soft x-ray absorption spectroscopies. The spectra exhibit strong variations with temperature. The energy gap is reduced by about 0.6 eV in going from 80 to 650 K but the near Fermi level intensity remains small, classifying $LaCoO_3$ as a bad metal even in the metallic phase. We are able to explain the spectra in terms of incoherent sums of low-spin and high-spin Co^{3+} spectra. We also find that the energy parameters for the two Co sites are very different, revealing that paramagnetic $LaCoO_3$ is a highly inhomogeneous system with local lattice relaxations that are spin-state-specific. This, in turn, provides a natural explanation for the much-debated temperature dependence of the activation energy for the transitions.

DOI: 10.1103/PhysRevX.13.011037

Subject Areas: Condensed Matter Physics, Magnetism, Strongly Correlated Materials

I. INTRODUCTION

$LaCoO_3$ has been the subject of an intense and continuous investigation for more than 50 years now. It shows an intriguing gradual transformation from a nonmagnetic insulator at low temperatures to a paramagnetic semiconductor above approximately 50–100 K, followed by an insulator-to-metal transition at around 450–550 K [1,2]. The nature of these transitions is the topic of long-standing and ongoing discussions [3–9] and Co-oxide-based materials are of relevance not only for the research field of basic solid state physics but also for the more application-oriented battery [10,11] and catalysis research [12,13].

It was long speculated that $LaCoO_3$ in the paramagnetic phase is an inhomogeneous spin-state system in which the nonmagnetic low-spin (LS) Co^{3+} ions and the magnetic high-spin (HS) may even form an ordered state [14,15], perhaps on a short-ranged dynamical scale [16]. This speculation is based on the notion that the effective ionic radius of LS Co^{3+} is smaller than that of HS Co^{3+} [17,18]. This can be understood as follows. Figure 1 displays the ionic $3d$ charge density of these Co^{3+} ions, with the LS ones having the t_{2g}^6 configuration (left) and the HS ones the $t_{2g}^4 e_g^2$ (right). The t_{2g} electron density is shown in blue and the e_g in yellow. For the CoO_6 octahedra in $LaCoO_3$, the steric repulsion between the Co and O along the bond axes will be larger if the e_g orbitals are occupied in comparison to a situation where there are no e_g electrons present. One can, therefore, expect that the Co—O bond lengths will strongly depend on the spin state of the Co.

Structural studies, however, are not able to detect the presence of such an ordering or even the presence of Co sites that have different bond lengths in the paramagnetic state [19–24]. Most of the experimental and theoretical investigations on the electronic structure of $LaCoO_3$, therefore, assume equivalent Co atoms [4,6,9] or spin-state inequivalent Co atoms based on purely electronic grounds [7,8,25–30].

Although there is no direct proof so far for the presence of structurally different Co sites, this does not mean that this issue can be put aside. The temperature dependence of the spin-state transition is still an unresolved problem. An x-ray absorption study at the Co $L_{2,3}$ edge [5] infers that the activation energy for the spin-state transition is not constant but increases gradually with temperature. This finding is neglected or even contested by more recent

*Present address: Diamond Light Source, Harwell Campus, Didcot OX11 0DE, Oxon, United Kingdom.

†Present address: Helmholtz-Zentrum Berlin für Materialien und Energie GmbH, Albert-Einstein-Straße 15, 12489 Berlin, Germany.

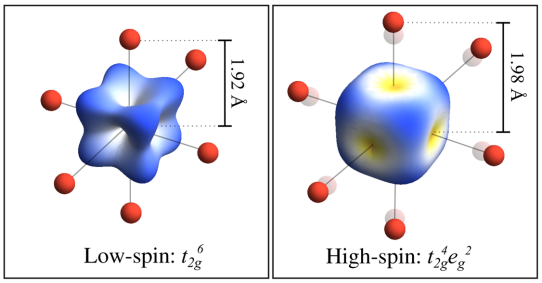

FIG. 1. Local ionic Co^{3+} $3d$ charge density in the CoO_6 octahedron: low spin with the t_{2g}^6 configuration (left) and high spin with the $t_{2g}^4 e_g^2$ (right). The electron density for the t_{2g} is displayed in blue and for the e_g in yellow. Red dots indicate the positions of the oxygens (faint red dots in the right denote the low spin positions).

studies [6–8,27–29] mainly on the basis that the lattice constant increases with temperature [23] so that the higher spin state would come lower in energy, meaning that the activation energy should decrease rather than increase with temperature. However, the presence of structurally different Co sites would provide a natural explanation for the increase of the activation energy with temperature and is obviously also of high relevance for the conductivity of $LaCoO_3$ in the metallic phase.

Here, we report our spectroscopy study on $LaCoO_3$ over a wide temperature range in the search for electronic signatures for the presence of structurally different Co sites associated with the different spin states. To this end, we carry out bulk-sensitive hard x-ray photoelectron spectroscopy (HAXPES) and x-ray absorption (XAS) at the O-K edge in combination with configuration-interaction calculations. Thanks to the increased bulk sensitivity, we are able to observe a very strong temperature dependence and to obtain spectra with details that have not been observed so far [31–36]. We find not only that the spectra can be well explained by an incoherent sum of LS and HS spectra, but, above all, also that the two Co sites have very different energy parameters, indicative of the presence of spin-specific local lattice relaxations.

II. METHODS

The HAXPES experiments are carried out at the Max-Planck-NSRRC HAXPES end station at the Taiwan undulator beam line BL12XU at SPring-8, Japan. The photon beam is linearly polarized with the electrical field vector in the plane of the storage ring (i.e., horizontal), and the photon energy is set at about 6.5 keV. An MB Scientific A-1 HE analyzer, mounted vertically, is used [37]. The photoelectrons are collected in the direction perpendicular to the electrical field vector of the photon beam. The overall energy resolution is set at around 0.35 eV, and the Fermi level is calibrated using polycrystalline silver. The O-K XAS measurements are performed at the Dragon beam line of the National Synchrotron Radiation Research Center (NSRRC) in Taiwan with an energy resolution of 0.25 eV. The spectra are recorded using the total fluorescence yield method. XAS spectra of NiO are also measured for energy calibration. The XAS spectra are normalized to the average spectral intensity in the energy range 556–570 eV.

Single crystals of 0.2% Sr-doped $LaCoO_3$ are grown by the traveling floating-zone method in an image furnace. The magnetic susceptibility is measured using a Quantum Design vibrating sample magnetometer, reproducing the data reported earlier [38–40]. The small Sr doping reduces the resistivity, allowing us to minimize the charging effects that are known to affect photoemission spectra at very low temperatures [35]. Our HAXPES spectra collected at 80 K show only a rigid energy shift (0.98 eV) toward higher binding energy without any sign of distortion. This energy shift is corrected by aligning the O $1s$ spectrum to the spectra measured at higher temperatures. The spectra are normalized to the total integrated intensity after the background due to secondary electrons is subtracted. Clean sample surfaces are obtained by cleaving the samples *in situ* in an ultrahigh vacuum preparation chamber with a pressure in the 10^{-10} mbar range.

Full atomic-multiplet configuration-interaction calculations including crystal field interactions as well as the Co $3d - O\ 2p$ hybridization are performed for a CoO_6 cluster using the XTLS9.25 code [41]. The parameters used are close to earlier work [5] and discussed in further detail in the text and Appendix [42]. A combination of Gaussian and Lorentzian broadening is applied to compare the calculations with the experimental spectra. The spin state is stabilized by choosing different crystal field values [5,42]. In the Appendix, we explain in detail that the difference in the chosen $10Dq$ parameters is large enough to obtain the pure LS and HS states and yet small enough to have quite similar total electronic energies. In order to reproduce the spectra at elevated temperatures, the HS calculations are performed with a 15% reduction of the hybridization integrals to account for local lattice relaxations. The effect of this reduction is discussed in further detail in the following sections.

III. RESULTS

In Fig. 2, we display the HAXPES spectra of the Co $2p$ and O $1s$ core levels of $LaCoO_3$ at different temperatures. The Co $2p$ core-hole spin-orbit coupling splits the spectrum roughly in two parts, namely, the Co $2p_{3/2}$ (main line at approximately 780 eV binding energy and charge transfer satellite at approximately 790 eV) and Co $2p_{1/2}$ (main line at approximately 795 eV and charge transfer satellite at approximately 805 eV). The spectra show strong changes with temperature. At 80 K, the Co $2p_{3/2}$ main line is quite narrow. As the temperature is increased, the main lines become very broad and very asymmetric. One could

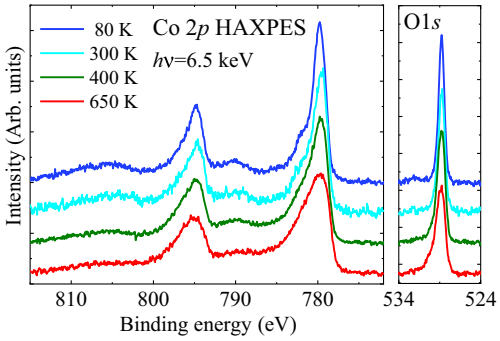

FIG. 2. Co $2p$ (left) and O $1s$ (right) HAXPES spectra of $LaCoO_3$ measured at different temperatures.

argue that this strong change in shape of the Co $2p$ spectrum is simply a temperature broadening effect. However, looking at the temperature evolution of the O $1s$ spectrum, one can observe that the broadening here is much smaller than in the Co $2p$. At high temperatures, the O $1s$ line also exhibits an increased asymmetry, but this is not comparable with that of the Co $2p$ spectrum. For the O $1s$, it simply reflects the increased amount of electron-hole pair excitations accompanying the core-hole creation upon entering the high-temperature metallic phase [43].

In order to explain the temperature evolution of the Co $2p$ spectrum quantitatively, we perform configuration-interaction calculations using a CoO_6 cluster. Figure 3(a) depicts the Co $2p$ spectrum for the LS state and Fig. 3(f) for the HS state. These results are very close to those of Hariki, Yamanaka, and Uozumi using a dynamical mean field theory based on the Anderson impurity model [44]. The LS and HS spectral line shapes are quite different. In an attempt to simulate the experimental spectra taken at 80 K [see Fig. 3(b)] and at 650 K [see Fig. 3(e)], we take the temperature-dependent spin-state occupations as inferred from the earlier XAS study [5] and construct an incoherent sum of the LS and HS spectra accordingly. Figure 3(c) displays the 90% LS and 10% HS sum which reproduces very well the experimental 80 K spectrum. Figure 3(d) shows the 50% LS and 50% HS sum which matches also very satisfactorily the experimental 650 K spectrum. Figure 3, thus, demonstrates that we can obtain a quantitative understanding of the spin-state transition in $LaCoO_3$ from the Co $2p$ core-level HAXPES. These HAXPES findings are fully consistent with those of the Co $L_{2,3}$ XAS [5]. Here, we note that we perform the HS calculations with and without the 15% hybridization reduction in order to model the presence or absence, respectively, of lattice relaxations as explained below. For the analysis of the Co $2p$ spectra, the outcome is not sensitive to this hybridization reduction, since the lifetime broadening of the Co $2p$ is quite large. For completeness, we mention that the HS calculations depicted in Fig. 3 include the hybridization reduction.

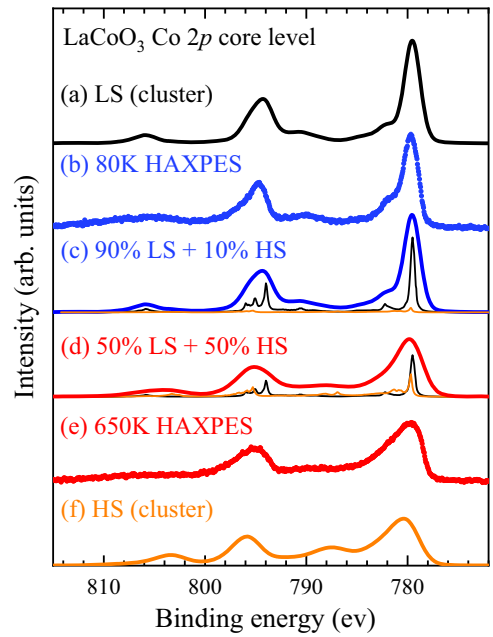

FIG. 3. (a),(f) Full-multiplet configuration-interaction cluster calculations of the LS (HS) Co $2p$ photoemission spectra of $LaCoO_3$. (b),(e) Co $2p$ HAXPES experimental spectra at 80 K (650 K). (c),(d) Theoretical simulation of the Co $2p$ spectra at 80 K (650 K). The simulation uses an incoherent sum of the calculated LS and HS spectra with a ratio of 90% LS and 10% HS (50% LS and 50% HS). The spectra are normalized to the integrated total intensity. The thin lines are calculations with reduced broadening of the LS and HS components, with the overall intensity divided by a factor of 5 for clarity.

The top in Fig. 4 shows the valence band HAXPES spectrum of $LaCoO_3$ as a function of the temperature. The temperature dependence can be observed most clearly in the peak at 0.8 eV binding energy. In order to interpret the spectral features, we first focus on the low-temperature

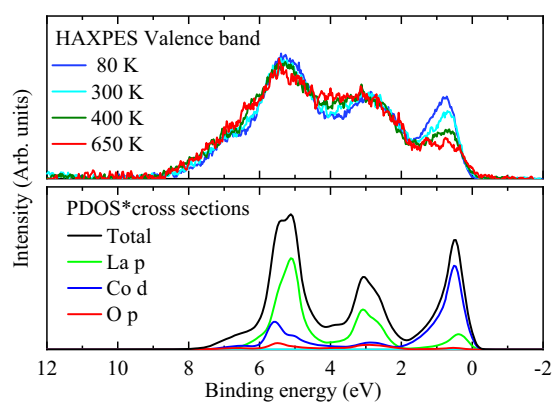

FIG. 4. Top: valence band HAXPES spectra of $LaCoO_3$ taken at different temperatures. Bottom: simulation using the local-density approximation (LDA) partial density of states of the Co $3d$, O $2p$, and La $5p$ multiplied with their respective photoionization cross sections, reproduced from Ref. [45].

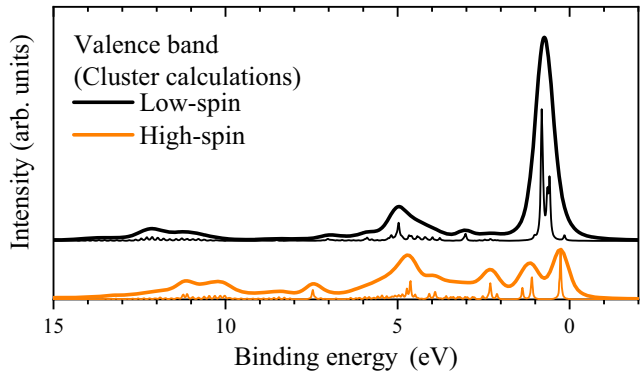

FIG. 5. Configuration-interaction calculations of the Co $3d$ photoemission spectrum of $LaCoO_3$ starting from the LS and HS initial states, normalized to the integrated total intensity. Thin lines are calculations with reduced broadening, with the intensity divided by a factor of 5 for clarity.

spectrum. $LaCoO_3$ is then a nonmagnetic insulator, with the Co^{3+} $3d^6$ ion having the low-spin t_{2g}^6 configuration. Despite the presence of strong electronic correlations, nonmagnetic $LaCoO_3$ with a completely filled t_{2g} and empty e_g subshells can effectively be considered as a band insulator, for which *ab initio* band structure calculations can provide a reasonable description of its electronic structure. Indeed, analysis on the basis of partial density of states multiplied by their respective photoionization cross sections yields highly satisfactory results [45]. These results are reproduced in the bottom in Fig. 4. We can observe that the HAXPES valence band spectrum is dominated by the La $5p$, except for the peak at 0.8 eV, for which the Co $3d$ gives the largest contribution. The fact that this 0.8 eV peak also shows the strongest temperature dependence tells us that we can make use of it for our study of the local Co $3d$ electronic structure across the spin-state and insulator-to-metal transitions.

In order to capture the Co $3d$ photoemission spectrum beyond the mean field approach, we perform configuration-interaction calculations for both the LS and the HS initial states. The results are displayed in Fig. 5. We can observe that, for the LS initial state, the Co $3d$ spectrum between 0 and 8 eV is quite similar to the Co $3d$ LDA partial density of states from Fig. 4, proving that the LS state is effectively a band semiconductor. The 0.8 eV peak can be assigned to a $t_{2g}^6 + h\nu \rightarrow t_{2g}^5 + e$ photoemission process, which is the analog of the LDA t_{2g} partial density of states. Only for high energies, i.e., between 10 and 14 eV, can one observe signatures (verified also in a soft x-ray photoemission experiment [46]) of correlation effects that are absent in the LDA approach. In contrast, the photoemission spectrum for the HS initial state with the $t_{2g}^4 e_g^2$ configuration has no LDA analog. It consists of several atomic multiplet structures, which cannot be explained within the LDA approach. Most significant is that the 0.8 eV peak of the LS spectrum is no longer there or, rather, distributed over a wide range of energies in case the initial state is HS. The experimentally observed suppression of the 0.8 eV peak with temperature in Fig. 4 is, therefore, signaling the LS-HS transition, consistent with the Co $2p$ core-level data shown in Fig. 3. Here, we note that the scenario of a spin-state transition from the LS to the intermediate spin (IS) is not compatible with the temperature evolution of the experimental valence band spectra; see the Appendix for a detailed line-shape analysis.

Having established the general features of the electronic structure of $LaCoO_3$ across the spin-state transition, we now focus on the electronic states closest to the Fermi level. The top left in Fig. 6 shows a close-up of the near E_F valence band HAXPES spectrum. The strong suppression of the 0.8 eV photoemission peak with increasing temperature can be clearly seen. Remarkable is that the intensity at the Fermi level remains small at all temperatures, i.e., even at 650 K where $LaCoO_3$ is deep in the metallic phase. This indicates that $LaCoO_3$ should be classified as a bad metal after passing the gradual insulator-to-metal transition.

The top right in Fig. 6 displays the pre-edge region of the O-K XAS. The spectral structures from 527 to 531 eV are due to transitions from the O $1s$ core level to the O $2p$ orbitals that are mixed with the unoccupied Co $3d$ t_{2g} and e_g states [47]. We can observe a strong transfer of spectral weight from the higher-energy structure at around 529.3 eV to the lower-energy one at around 528.4 eV when increasing the temperature from 10 to 650 K. This is a manifestation of the spin-state transition and can be explained as follows. At low temperatures, the LS Co^{3+} ion has its t_{2g} shell completely occupied [5], and only transitions to the higher-lying empty e_g states are possible. At higher temperatures, with part of the Co ions in the HS state [5], the t_{2g} states become partially unoccupied so that then transitions to the lower-lying t_{2g} states are also allowed, leading to the appearance of the 528.4 eV structure. As the temperature increases, this lower-energy structure gains gradually spectral weight at the expense of the higher-energy one. Thereby, the leading edge of the O-K XAS gets lowered by about 0.6 eV, indicating the reduction of the band gap [38] due to the presence of HS Co.

IV. DISCUSSION

To interpret quantitatively the above low-energy features of the electronic structure, we perform detailed configuration-interaction calculations, not only for the photoemission spectrum but also for the inverse photoemission, i.e., the states on both sides of the Fermi level. Here, we note that the pre-edge region of the O-K XAS can be considered as a good approximation for the inverse photoemission spectrum as far as the relative energy positions of the spectral features are concerned [48]. The bottom in Fig. 6 displays the photoemission and inverse photoemission

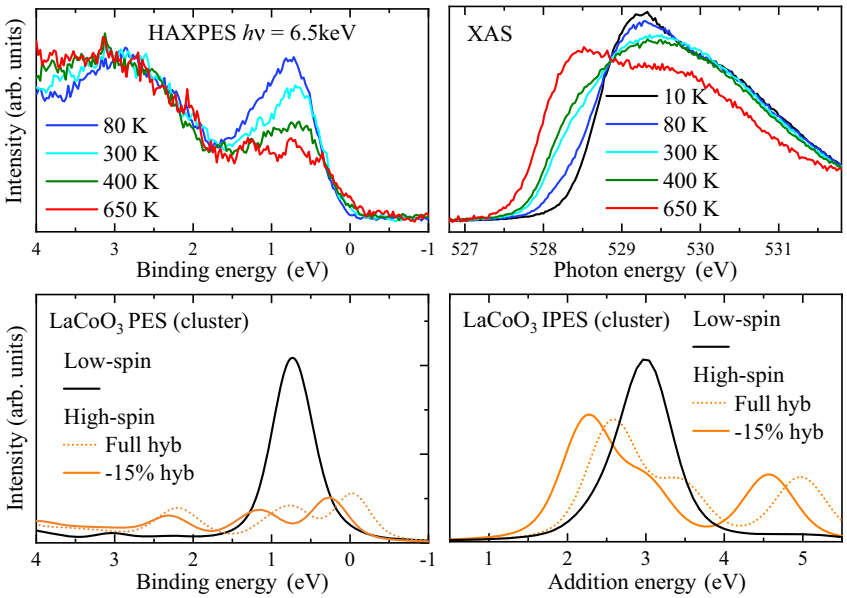

FIG. 6. Top: close-up of the valence band HAXPES (top left) and the pre-edge region of the O-K XAS (top right) spectra of $LaCoO_3$ at different temperatures. Bottom: configuration-interaction calculations of the Co $3d$ photoemission (PES, bottom left) and inverse photoemission spectra (IPES, bottom right) using $10Dq = 0.75$ (0.40) eV for the LS (HS) state. The HS calculations are performed with (solid line) and without (dotted line) the hybridization reduction to model the presence or absence, respectively, of local lattice relaxations.

spectra calculated for the CoO_6 cluster in the LS (black solid lines) and HS (orange dashed and solid lines) states.

We first discuss the scenario that represents a situation without local lattice relaxations, i.e., an inhomogeneous spin-state situation based on purely electronic grounds. To this end, we calculate the LS and HS spectra using the same hybridization integral values, i.e., without the hybridization reduction in the HS calculations. The results are shown in the bottom in Fig. 6 by the solid black lines for the LS and by the orange dashed lines for the HS. We can observe that the calculated HS spectra are quite off in energy with respect to the experiment. Having the photoemission main peak of the LS located at 0.8 eV binding energy, this HS spectrum has strong intensities at the Fermi level, in clear disagreement with the experiment. For the inverse photoemission (and, thus, the O-K) spectrum, the difference between the calculated LS main peak (located at 3 eV) and the HS main peak (2.5 eV) is 0.5 eV, while the experiment shows that the energy distance is about 0.9 eV (529.3 vs 528.4 eV).

In order to resolve the discrepancy between the experiment and the results from the model with a purely electronic spin-state inhomogeneity, we now explicitly assume that there is a sufficiently significant difference in the energy parameters between the LS and HS sites. It is found from neutron diffraction [23] that the Co-O distance in $LaCoO_3$ is 1.925 Å at 5 K and 1.949 Å at 650 K. These distances are extracted assuming a single Co site in the crystal. We now infer that there are two Co-O distances at 650 K, one to be associated with the LS Co and the other with the HS Co. With a 50%–50% LS-HS distribution at 650 K [5], we may assign a Co-O distance of approximately 1.92 Å for the LS Co (from the 5 K data) and approximately 1.98 Å for the HS Co, as illustrated in Fig. 1, thereby keeping the average at the reported value of 1.949 Å. We note that our Co—O bond length difference between the LS and HS states is well within the limits found from an EXAFS study [24]. An analysis of the thermal expansion data assuming an inhomogeneous mixture of LS and HS sites also yields a Co-O distance difference in the few percent range [49]. Such a difference in the Co-O distance directly results in a large difference in the Co-O hybridization (hopping) integral [50]. We estimate that the Co-O hybridization integral for the HS Co could be about 15% smaller than for the LS Co.

We, thus, calculate the photoemission and inverse photoemission spectra for the HS CoO_6 cluster with the hybridization integral reduced by 15%. The results are shown by the orange solid lines in the bottom in Fig. 6. We can observe that the photoemission spectrum is moved to higher binding energies and the inverse photoemission to lower addition energies by about 0.5 eV in comparison to the scenario with unreduced hybridization. The match with the experimental spectra are now much improved: The calculated spectral features are at the correct energy positions. Our findings of such peak shifts are not inconsistent with earlier theoretical model calculations that include the breathing-type local lattice relaxations [51,52].

We, thus, find evidence from the local electronic structure that the LS and HS Co ions have quite different oxygen

environments: The differences in the hybridization (hopping) integrals can be assigned to differences in the Co-O distances. The presence of these spin-state-specific local lattice relaxations is crucial to understand the gradual spin-state transition in Co oxide materials. It is found from XAS that the LS-HS activation energy increases with temperature [5]. As already mentioned above, this finding is questioned by later studies [6–9,27–29] on the basis that the lattice constant increases with temperature [23] so that one would rather expect that the activation energy decreases with temperature, since larger Co-O distances means weaker crystal or ligand fields and, thus, lower energies for the HS state. We note, however, the following point: Once the LS-HS occupations and their temperature dependence are measured experimentally, as the XAS study does [5] and now also our present study, then inevitably also the temperature dependence of the LS-HS activation energy is implicitly determined. So, rather than questioning whether the activation energy increases with temperature, one should pose the question why. We can now answer this why question.

The thermal expansion of $LaCoO_3$ can be attributed to two different effects. One is due to phonons. The other is due to the LS-HS transition where the average Co-O distances increase [23,39] when more of the larger HS Co ions become present. Enlargement of the local Co-O distances due to phonons indeed leads to a lowering of the crystal or ligand field and, thus, also a lowering of the activation energy. However, thermal expansion due to the LS-HS transition does not necessarily mean that the Co-O distances of LS Co ions or those of HS Co ions are increased with temperature. In fact, since lattice expansion costs energy, one could readily envision that the Co-O distances for a LS Co ion get decreased if it is surrounded at elevated temperatures by HS instead of LS Co ions and that it becomes also more difficult to find space to accommodate a newly created HS Co if it is surrounded by HS instead of LS Co ions. Thus, the more the LS-HS transition progresses, the more energy it takes to convert the next LS to a HS ion. We also note that analysis of neutron diffraction data finds that the LS-HS transition (and not the phonons) plays the dominant role in the thermal expansion in the low-temperature regime that extends up to 400 K [23]. This implies that in this regime the activation energy is expected to increase with higher temperatures. This is, in fact, what actually is extracted from the Co $L_{2,3}$ XAS data [5], namely, a continuous increase of the activation energy from 20 to 400 K, followed by a regime of constant activation energy for temperatures above 400 K.

We stress that the above considerations are, of course, possible only if one recognizes the presence of spin-state-specific Co-O distances, the justification of which is being provided by our new spectroscopic data and the analysis thereof. The presence of spin-state-specific Co-O distances provides also an additional explanation of the bad metal behavior of $LaCoO_3$ in the metallic phase, since the conductivity is affected by the small polaron formation. Finally, in an attempt to explain the absence of a LS-HS ordering at elevated temperatures and the temperature dependence of the HS excitation energy, Hariki *et al.* propose a model with the intermediate-spin excitations which couple to the HS excitations [30]. It would be interesting to also include the effect of local lattice relaxations in this model.

V. CONCLUSION

In summary, we have acquired photoemission and x-ray absorption spectra that are representative for bulk $LaCoO_3$. The spectra exhibit strong variations across the gradual spin-state and insulator-to-metal transitions. A reduction of the band gap can be observed with increasing temperature but the near Fermi level intensity remains small even in the metallic phase. The spectra can be explained quantitatively in terms of incoherent sums of low-spin and high-spin Co^{3+} spectra, thereby revealing that the energy parameters for the two Co sites are very different. The spin-state inhomogeneity of paramagnetic $LaCoO_3$ involves strong local lattice relaxations that are spin-state-specific. The presence of these lattice relaxations is a necessary ingredient to explain the temperature dependence of the activation energy of the spin-state transition.

ACKNOWLEDGMENTS

The research in Cologne and Dresden was partially supported by the Deutsche Forschungsgemeinschaft through SFB 608, FOR 1346, and SFB 1143 (Project-ID No. 247310070). We acknowledge support from the Max Planck-POSTECH-Hsinchu Center for Complex Phase Materials.

APPENDIX A: CLUSTER CALCULATIONS

The configuration-interaction calculations are performed using an octahedral CoO_6 cluster with parameters as described by Haverkort *et al.* [5] and listed in Ref. [42]. The calculations include the full atomic multiplet theory and the spin-orbit interaction in the Co $2p$ and Co $3d$ shells as well as the Co-O hybridization and the ionic crystal electric field $10Dq$. The LS and HS calculations are carried out using different values of the ionic crystal electric field: $10Dq = 0.75$ eV is taken to obtain the LS ground state and $10Dq = 0.40$ eV for the HS ground state. These two parameter values are chosen such that they are on the opposite sides of the LS-HS transition and yet not too close to this LS-HS crossing, which otherwise would have led to a mixing between the LS and HS states due to the Co $3d$ spin-orbit interaction [5]. Such a mixing would not be consistent with the experimentally recorded XAS spectra. The difference in the total energy of the two ground states

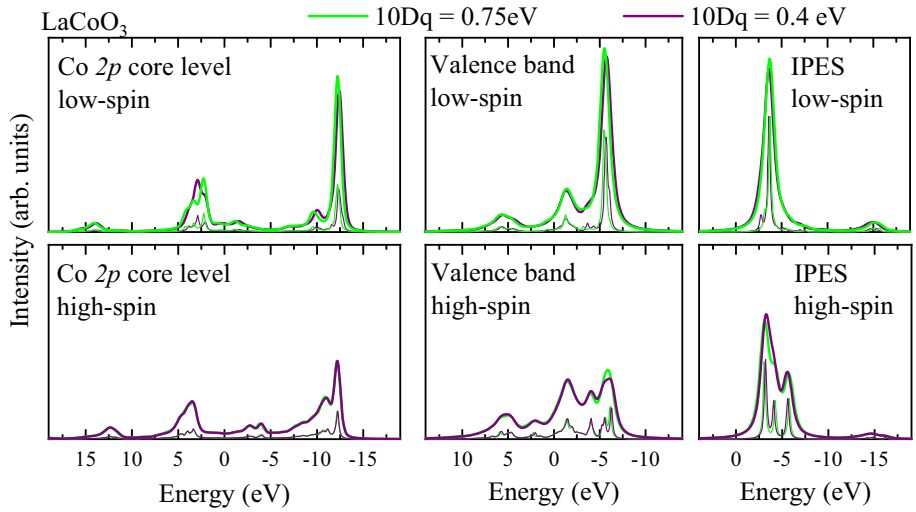

FIG. 7. Configuration-interaction calculations for the Co $2p$ core level, Co $3d$ valence band, and Co $3d$ inverse photoemission spectra using an octahedral CoO_6 cluster, starting from a low-spin (LS, top) and high-spin (HS, bottom) state of the Co^{3+}. For $10Dq = 0.75$ eV, the ground state is LS, and the excited states are HS. Their spectra are in green. For $10Dq = 0.40$ eV, the ground state is HS, and an excited state is LS. Their spectra are in purple. Thin lines are calculations with reduced broadening.

with $10Dq = 0.75$ eV and $10Dq = 0.40$ eV is about 0.1 eV, which is small in comparison with the bandwidth.

We investigate to what extent the choice of $10Dq = 0.75$ eV vs $10Dq = 0.40$ eV affects the spectra beyond the expected LS vs HS differences. To this end, we calculate the LS spectra from the LS ground state of the $10Dq = 0.75$ eV calculation and compare it with the LS spectra from the LS excited state of the $10Dq = 0.40$ eV. The results are plotted in the top in Fig. 7: green lines for the $10Dq = 0.75$ eV cluster and purple lines for the $10Dq = 0.40$ eV. We can observe that the LS spectra of the two different clusters have quite similar line shapes and energy positions. We also calculate the HS spectra using the HS ground state of the $10Dq = 0.40$ eV cluster and the HS spectra from the HS excited state of the $10Dq = 0.75$ eV. In order to observe only the effect of changing $10Dq$, the hybridization parameter is not reduced for the HS in this exercise. The bottom in Fig. 7 shows that also here the purple and green lines almost fall on top of each other. We, therefore, can safely conclude that the differences between the LS and HS spectra, i.e., the difference between the top and bottom in Fig. 7, are much larger than the tiny differences caused by the precise value of the $10Dq$ parameter, i.e., the differences between the green and purple lines inside each panel.

1. Low-spin to intermediate-spin transition?

Here, we investigate whether the LS to IS scenario is also compatible with the temperature evolution of the experimentally acquired spectra.

In Fig. 8(a), we display the 650 K HAXPES valence band spectrum (solid red curve) together with the Co $3d$ spectral weight from the cluster calculations for the Co ion in the intermediate spin with full hybridization (solid magenta line) and with 15%-reduced hybridization (dashed magenta line). Here, we note that at any given temperature the amount of IS in the LS-IS scenario must be twice that of HS in the LS-HS in order to reproduce the experimentally observed magnetic susceptibility signal, recalling that the magnetic moment of the IS is half of the HS. This means that, at 650 K, we have a 0%–100% LS-IS occupation instead of the 50%–50% LS-HS put forward in the present manuscript. In other words, the 650 K spectrum should be compared directly with the calculated IS spectral weight. We can observe that there is an obvious and very large discrepancy between the experiment and the IS simulation. In Fig. 8(b), we show the pre-edge region of the 650 K O-K XAS spectrum $LaCoO_3$ (red line) together with the calculated Co $3d$ inverse photoemission spectrum in the IS state (IPES, magenta line). Also, here we notice that the IS simulation has a different line shape than the experiment.

To reconfirm the validity of the LS-HS scenario, we look in more detail into the temperature evolution of the HAXPES valence band spectra. In Fig. 9(a), we display the 80 (solid blue curve) and 650 K (solid red curve) spectra together with the Co $3d$ partial density of states from the band structure calculations (LDA) in the nonmagnetic, low-spin state (LS, solid black curve) as well as the Co $3d$ spectral weight from the cluster calculations for the Co ion in the high-spin state (HS, solid brown line). In Fig. 9(b), we show the temperature evolution of the measured spectra by plotting the difference between the 650 and 80 K HAXPES spectra (solid purple line). We now compare this experimental result with the LS-HS scenario as used in the present manuscript. We, thus, calculate the 80 K spectrum as the sum of the 90% LS and 10% HS spectra and the 650 K spectrum as the sum of 50% LS and 50% HS.

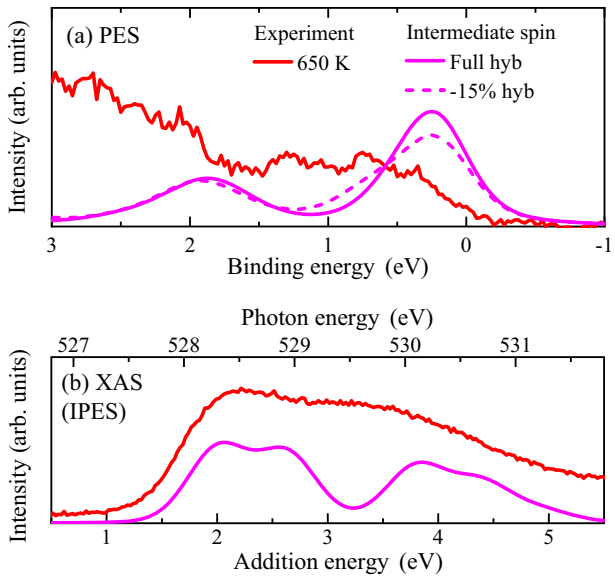

FIG. 8. (a) Close-up of the 650 K valence band HAXPES (red line) overlapped with the intermediate-spin cluster calculation with full (solid magenta line) and reduced (dashed magenta line) hybridization. (b) The pre-edge region of the O-*K* XAS spectrum of $LaCoO_3$ at 650 K (red line) together with the cluster calculation of the Co 3*d* inverse photoemission spectrum (IPES, magenta line) for the intermediate-spin state.

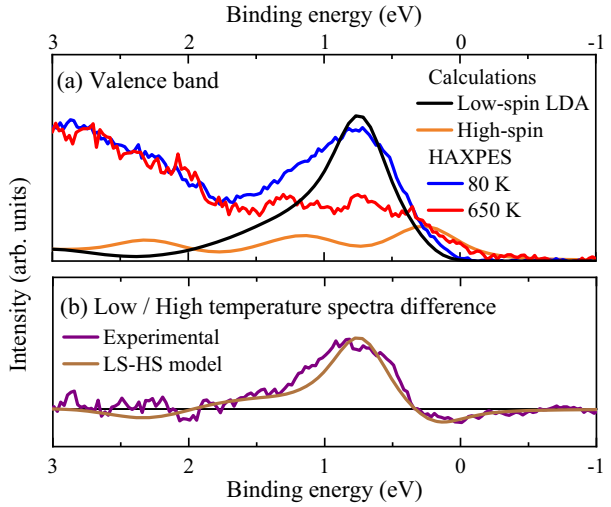

FIG. 9. (a) Close-up of the 80 (blue line) and 650 K (red line) valence band HAXPES overlapped with the low-spin LDA calculations (black line) [45] and the high-spin cluster calculation (brown line). (b) Difference between the 80 and 650 K experimental spectra (purple line) and the simulated difference using the low-spin and high-spin (LS-HS) model (brown line).

The difference between the calculated 650 and 80 K spectra is depicted in Fig. 8(b) (solid brown curve). The match between the experiment and the LS-HS scenario is very satisfactory.

We, thus, can firmly conclude that the LS-HS scenario explains the temperature evolution of the experimental spectra of $LaCoO_3$, while the LS-IS model is not compatible with the measured data. The sensitivity of this analysis can be traced back to the very different line spectral shapes of the LS, IS, and HS states and to the very different amount of spin-configuration occupations at 650 K, namely, 50%–50% for LS-HS and 0%–100% for LS-IS.

[1] R. R. Heikes, R. C. Miller, and R. Mazelsky, *Magnetic and Electrical Anomalies in* $LaCoO_3$, Physica (Utrecht) **30**, 1600 (1964).

[2] G. Blasse, *Magnetic Properties of Mixed Metal Oxides Containing Trivalent Cobalt*, J. Appl. Phys. **36**, 879 (1965).

[3] P. M. Raccah and J. B. Goodenough, *First-Order Localized-Electron ⇆ Collective-Electron Transition in* $LaCoO_3$, Phys. Rev. **155**, 932 (1967).

[4] M. A. Korotin, S. Yu. Ezhov, I. V. Solovyev, V. I. Anisimov, D. I. Khomskii, and G. A. Sawatzky, *Intermediate-Spin State and Properties of* $LaCoO_3$, Phys. Rev. B **54**, 5309 (1996).

[5] M. W. Haverkort, Z. Hu, J. C. Cezar, T. Burnus, H. Hartmann, M. Reuther, C. Zobel, T. Lorenz, A. Tanaka, N. B. Brookes, H. H. Hsieh, H.-J. Lin, C. T. Chen, and L. H. Tjeng, *Spin State Transition in* $LaCoO_3$ *Studied Using Soft X-Ray Absorption Spectroscopy and Magnetic Circular Dichroism*, Phys. Rev. Lett. **97**, 176405 (2006).

[6] R. Eder, *Spin-State Transition in* $LaCoO_3$ *by Variational Cluster Approximation*, Phys. Rev. B **81**, 035101 (2010).

[7] M. Karolak, M. Izquierdo, S. L. Molodtsov, and A. I. Lichtenstein, *Correlation-Driven Charge and Spin Fluctuations in* $LaCoO_3$, Phys. Rev. Lett. **115**, 046401 (2015).

[8] K. Tomiyasu, J. Okamoto, H. Y. Huang, Z. Y. Chen, E. P. Sinaga, W. B. Wu, Y. Y. Chu, A. Singh, R.-P. Wang, F. M. F. de Groot, A. Chainani, S. Ishihara, C. T. Chen, and D. J. Huang, *Coulomb Correlations Intertwined with Spin and Orbital Excitations in* $LaCoO_3$, Phys. Rev. Lett. **119**, 196402 (2017).

[9] Bismayan Chakrabarti, Turan Birol, and Kristjan Haule, *Role of Entropy and Structural Parameters in the Spin-State Transition of* $LaCoO_3$, Phys. Rev. Mater. **1**, 064403 (2017).

[10] K. Mizushima, P. C. Jones, P. J. Wiseman, and J. B. Goodenough, Li_xCoO_2 *($0 < x < -1$): A New Cathode Material for Batteries of High Energy Density*, Mater. Res. Bull. **15**, 783 (1980).

[11] M. Stanley Whittingham, *Lithium Batteries and Cathode Materials*, Chem. Rev. **104**, 4271 (2004).

[12] Jin Suntivich, Kevin J. May, Hubert A. Gasteiger, John B. Goodenough, and Yang Shao-Horn, *A Perovskite Oxide Optimized for Oxygen Evolution Catalysis from Molecular Orbital Principles*, Science **334**, 1383 (2011).

[13] Jing Zhou, Linjuan Zhang, Yu-Cheng Huang, Chung-Li Dong, Hong-Ji Lin, Chien-Te Chen, L. H. Tjeng, and Zhiwei Hu, *Voltage- and Time-Dependent Valence State Transition in Cobalt Oxide Catalysts during the Oxygen Evolution Reaction*, Nat. Commun. **11**, 1984 (2020).

[14] John B. Goodenough, *An Interpretation of the Magnetic Properties of the Perovskite-Type Mixed Crystals* $Li_{1-x}Sr_xCoO_{3-\lambda}$, J. Phys. Chem. Solids **6**, 287 (1958).

[15] J. B. Goodenough and P. M. Raccah, *Complex vs Band Formation in Perovskite Oxides*, J. Appl. Phys. **36**, 1031 (1965).

[16] M. A. Señarís-Rodríguez and J. B. Goodenough, $LaCoO_3$ *Revisited*, J. Solid State Chem. **116**, 224 (1995).

[17] R. D. Shannon and C. T. Prewitt, *Effective Ionic Radii in Oxides and Fluorides*, Acta Crystallogr. Sect. B **25**, 925 (1969).

[18] R. D. Shannon, *Revised Effective Ionic Radii and Systematic Studies of Interatomic Distances in Halides and Chalcogenides*, Acta Crystallogr. Sect. A **32**, 751 (1976).

[19] G. Thornton, B. C. Tofield, and D. E. Williams, *Spin State Equilibria and the Semiconductor to Metal Transition of* $LaCoO_3$, Solid State Commun. **44**, 1213 (1982).

[20] G. Thornton, B. C. Tofield, and A. W. Hewat, *A Neutron Diffraction Study of* $LaCoO_3$ *in the Temperature Range* $4.2 < T < 1248$ K, J. Solid State Chem. **61**, 301 (1986).

[21] Kichizo Asai, Osamu Yokokura, Nobuhiko Nishimori, Henry Chou, J. M. Tranquada, G. Shirane, Sadao Higuchi, Yuichiro Okajima, and Kay Kohn, *Neutron-Scattering Study of the Spin-State Transition and Magnetic Correlations in* $La_{1-x}Sr_xCoO_3$ *(*$x = 0$ *and 0.08)*, Phys. Rev. B **50**, 3025 (1994).

[22] Kichizo Asai, Atsuro Yoneda, Osamu Yokokura, J. M. Tranquada, G. Shirane, and Key Kohn, *Two Spin-State Transitions in* $LaCoO_3$, J. Phys. Soc. Jpn. **67**, 290 (1998).

[23] P. G. Radaelli and S.-W. Cheong, *Structural Phenomena Associated with the Spin-State Transition in* $LaCoO_3$, Phys. Rev. B **66**, 094408 (2002).

[24] N. Sundaram, Y. Jiang, I. E. Anderson, D. P. Belanger, C. H. Booth, F. Bridges, J. F. Mitchell, Th. Proffen, and H. Zheng, *Local Structure of* $La_{1-x}Sr_xCoO_3$ *Determined from EXAFS and Neutron Pair Distribution Function Studies*, Phys. Rev. Lett. **102**, 026401 (2009).

[25] Robert A. Bari and J. Sivardière, *Low-Spin-High-Spin Transitions in Transition-Metal-Ion Compounds*, Phys. Rev. B **5**, 4466 (1972).

[26] Min Zhuang, Weiyi Zhang, and Naiben Ming, *Competition of Various Spin States of* $LaCoO_3$, Phys. Rev. B **57**, 10705 (1998).

[27] Jan Kuneš and Vlastimil Křápek, *Disproportionation and Metallization at Low-Spin to High-Spin Transition in Multiorbital Mott Systems*, Phys. Rev. Lett. **106**, 256401 (2011).

[28] V. Křápek, P. Novák, J. Kuneš, D. Novoselov, Dm. M. Korotin, and V. I. Anisimov, *Spin State Transition and Covalent Bonding in* $LaCoO_3$, Phys. Rev. B **86**, 195104 (2012).

[29] Guoren Zhang, Evgeny Gorelov, Erik Koch, and Eva Pavarini, *Importance of Exchange Anisotropy and Superexchange for the Spin-State Transitions in* $rCoO_3$ *(*$r =$ rare earth*) Cobaltates*, Phys. Rev. B **86**, 184413 (2012).

[30] Atsushi Hariki, Ru-Pan Wang, Andrii Sotnikov, Keisuke Tomiyasu, Davide Betto, Nicholas B. Brookes, Yohei Uemura, Mahnaz Ghiasi, Frank M. F. de Groot, and Jan Kuneš, *Damping of Spinful Excitons in* $LaCoO_3$ *by Thermal Fluctuations: Theory and Experiment*, Phys. Rev. B **101**, 245162 (2020).

[31] L. Richter, S. D. Bader, and M. B. Brodsky, *Ultraviolet, X-Ray-Photoelectron, and Electron-Energy-Loss Spectroscopy Studies of* $LaCoO_3$ *and Oxygen Chemisorbed on* $LaCoO_3$, Phys. Rev. B **22**, 3059 (1980).

[32] A. Chainani, M. Mathew, and D. D. Sarma, *Electron-Spectroscopy Study of the Semiconductor-Metal Transition in* $La_{1-x}Sr_xCoO_3$, Phys. Rev. B **46**, 9976 (1992).

[33] M. Abbate, J. C. Fuggle, A. Fujimori, L. H. Tjeng, C. T. Chen, R. Potze, G. A. Sawatzky, H. Eisaki, and S. Uchida, *Electronic Structure and Spin-State Transition of* $LaCoO_3$, Phys. Rev. B **47**, 16124 (1993).

[34] S. R. Barman and D. D. Sarma, *Photoelectron-Spectroscopy Investigation of the Spin-State Transition in* $LaCoO_3$, Phys. Rev. B **49**, 13979 (1994).

[35] T. Saitoh, T. Mizokawa, A. Fujimori, M. Abbate, Y. Takeda, and M. Takano, *Electronic Structure and Temperature-Induced Paramagnetism in* $LaCoO_3$, Phys. Rev. B **55**, 4257 (1997).

[36] A. G. Thomas, W. R. Flavell, P. M. Dunwoody, C. E. J. Mitchell, S. Warren, S. C. Grice, P. G. D. Marr, D. E. Jewitt, N. Khan, V. R. Dhanak, D. Teehan, E. A. Seddon, Kichizo Asai, Yoshihiko Koboyashi, and Nobuyoshi Yamada, *Resonance Photoemission of* $LaCoO_3(111)$ *and* $La_{0.9}Sr_{0.1}CoO_3(111)$, J. Phys. Condens. Matter **12**, 9259 (2000).

[37] J. Weinen, T. C. Koethe, C. F. Chang, S. Agrestini, D. Kasinathan, Y. F. Liao, H. Fujiwara, C. Schüßler-Langeheine, F. Strigari, T. Haupricht, G. Panaccione, F. Offi, G. Monaco, S. Huotari, K.-D. Tsuei, and L. H. Tjeng, *Polarization Dependent Hard X-Ray Photoemission Experiments for Solids: Efficiency and Limits for Unraveling the Orbital Character of the Valence Band*, J. Electron Spectrosc. Relat. Phenom. **198**, 6 (2015).

[38] Y. Tokura, Y. Okimoto, S. Yamaguchi, H. Taniguchi, T. Kimura, and H. Takagi, *Thermally Induced Insulator-Metal Transition in* $LaCoO_3$*: A View Based on the Mott Transition*, Phys. Rev. B **58**, R1699 (1998).

[39] C. Zobel, M. Kriener, D. Bruns, J. Baier, M. Grüninger, T. Lorenz, P. Reutler, and A. Revcolevschi, *Evidence for a Low-Spin to Intermediate-Spin State Transition in* $LaCoO_3$, Phys. Rev. B **66**, 020402(R) (2002).

[40] M. Kriener, C. Zobel, A. Reichl, J. Baier, M. Cwik, K. Berggold, H. Kierspel, O. Zabara, A. Freimuth, and T. Lorenz, *Structure, Magnetization, and Resistivity of* $La_{1-x}M_xCoO_3$ *(*$m =$ Ca, Sr, *and* Ba*)*, Phys. Rev. B **69**, 094417 (2004).

[41] Arata Tanaka and Takeo Jo, *Resonant 3d, 3p and 3s Photoemission in Transition Metal Oxides Predicted at 2p Threshold*, J. Phys. Soc. Jpn. **63**, 2788 (1994).

[42] The parameters (in eV) used for the cluster calculations are $\Delta = 2.0$, $U_{dd} = 5.5$, $U_{pd} = 7.0$, $pd\sigma = -1.67$, and $pd\pi = 0.78$. $10Dq = 0.75$ is used for the low-spin calculations and $10Dq = 0.40$ for the high-spin calculations. Several ligand levels evenly placed within the energy width of 1 eV are included in order to consider the effects of the O $2p$ band dispersion. The high-spin calculations are performed with a 15% reduction of the hybridization integrals to account for local lattice relaxations. Slater integrals are reduced to 80% of the Hartree-Fock values, except for the spin-orbit coupling of the Co $2p$, which is reduced to 76% in order to match the experimentally observed splitting.

[43] S. Doniach and M. Sunjic, *Many-Electron Singularity in X-Ray Photoemission and X-Ray Line Spectra from Metals*, J. Phys. C **3**, 285 (1970).

[44] Atsushi Hariki, Akihiro Yamanaka, and Takayuki Uozumi, *Theory of Spin-State Selective Nonlocal Screening in* Co *2p X-Ray Photoemission Spectrum of* $LaCoO_3$, J. Phys. Soc. Jpn. **84**, 073706 (2015).

[45] D. Takegami, L. Nicolaï, T. C. Koethe, D. Kasinathan, C. Y. Kuo, Y. F. Liao, K. D. Tsuei, G. Panaccione, F. Offi, G. Monaco, N. B. Brookes, J. Minár, and L. H. Tjeng, *Valence Band Hard X-Ray Photoelectron Spectroscopy on* 3*d Transition-Metal Oxides Containing Rare-Earth Elements*, Phys. Rev. B **99**, 165101 (2019).

[46] Thomas Christoph Koethe, *Bulk Sensitive Photoelectron Spectroscopy of Strongly Correlated Transition Metal Oxides*, Ph.D. thesis, Universität zu Köln, 2006.

[47] Z. Hu, Hua Wu, T. C. Koethe, S. N. Barilo, S. V. Shiryaev, G. L. Bychkov, C. Schüßler-Langeheine, T. Lorenz, A. Tanaka, H. H. Hsieh, H.-J. Lin, C. T. Chen, N. B. Brookes, S. Agrestini, Y.-Y. Chin, M. Rotter, and L. H. Tjeng, *Spin-State Order/Disorder and Metal–Insulator Transition in* $GdBaCo_2O_{5.5}$*: Experimental Determination of the Underlying Electronic Structure*, New J. Phys. **14**, 123025 (2012).

[48] J. van Elp and Arata Tanaka, *Threshold Electronic Structure at the Oxygen K Edge of* 3*d-Transition-Metal Oxides: A Configuration Interaction Approach*, Phys. Rev. B **60**, 5331 (1999).

[49] K. Berggold, M. Kriener, P. Becker, M. Benomar, M. Reuther, C. Zobel, and T. Lorenz, *Anomalous Expansion and Phonon Damping due to the* Co *Spin-State Transition in* $RCoO_3$ *(*R = La, Pr, Nd, *and* Eu*)*, Phys. Rev. B **78**, 134402 (2008).

[50] W. A. Harrison, *Electronic Structure and the Properties of Solids* (Dover, New York, 1989).

[51] K. Knížek, Z. Jirák, J. Hejtmánek, and P. Novák, *Character of the Excited State of the* Co^{3+} *Ion in* $LaCoO_3$, J. Phys. Condens. Matter **18**, 3285 (2006).

[52] Karel Knížek, Zdeněk Jirák, Jiří Hejtmánek, Pavel Novák, and Wei Ku, GGA + *u Calculations of Correlated Spin Excitations in* $LaCoO_3$, Phys. Rev. B **79**, 014430 (2009).